

# MITIGATING EDGE EFFECTS IN ADHESIVELY BONDED COMPOSITE TUBULAR LAP JOINTS UNDER AXIAL, PRESSURE AND TORSIONAL LOADING VIA STIFFNESS-TAILORING

*M. A. Khan and S. Kumar*

*Institute Centre for Energy (iEnergy)  
Department of Mechanical and Materials Engineering,  
Masdar Institute of Science and Technology,  
P.O. Box 54224, Abu Dhabi, UAE*

**Keywords:** Composite joints, Adhesive bonding, Internal pressure, Torsion, Finite elements

## ABSTRACT

Adhesive bonding is the most preferred route for joining composites compared to traditional bolted and welded joints. Nevertheless, peak stress concentrations are generated near the ends of the bondline, which we refer to as an edge effect. These edge effects can be minimized by geometrically or materially grading the adherends in the joint region and /or grading the adhesive. Recent research suggests that the use of a compliant adhesive near the edge reduces the stress concentration while employing a stiff adhesive near the centre ensures sufficient load-transfer. Most of these works thus far concentrated on optimizing stress distribution in the joints subjected to axial and thermal loads. This study extends the idea of employing a bi-adhesive bondline to tubular joints experiencing torsional and pressure loads in addition to axial tension and bending. Single adhesive along the bondline was used as a baseline, while the joint with bi-adhesive along the bondline was used to optimise performance of joints. Finite element models of adhesively bonded composite tubular lap joints subjected to axial, pressure and torsional loading are developed. In case of pure axial loading, the dominant out-of-plane peak shear and radial stresses reduce by about 35% and 45% respectively in the presence of bi-adhesive bondline. For the case of pure internal pressure loading, peak shear, radial and hoop stresses reduces by about 45%, 40% and 50% respectively due to stiffness-tailoring. In-plane shear stress concentration in case of pure torsional loading reduces by about 30%.

## 1. INTRODUCTION

Fibre reinforced composites are extensively used in lightweight structural applications due to their high specific modulus / strength, better thermo-mechanical stability. Due to such inherent properties of composites, metallic piping in chemical, petrochemical and energy industry are being replaced by composites. Since such piping systems are subjected to harsh environmental load, corrosion also becomes extremely important. It is very well established that joints are the weakest links in piping assemblies and therefore it becomes very challenging to design and manufacture composite piping system especially with the limitation involved in fabrication of axisymmetric layered composites. Due to advancements in manufacturing techniques and low rotational inertia at relatively high stiffness compared to similar metallic shafts, composite shafts are very commonly used [1]. Large industry scale pipe assemblies are joined either mechanically or adhesively. Mechanical joints result in localized stress concentrations and damage which lowers the load carrying capacity of the joint as well as the structure itself. Therefore, in recent times adhesively glued joints are preferred over conventional mechanical joints. This extensive use of adhesive type bonding is due to ease of application, time and cost savings, high corrosion and fatigue resistance, crack retardance and good damping characteristics [1, 2].

Although the adhesively bonded tubular joints shows relatively superior load-transfer behaviour in relation to their conventional counterparts, peak stress concentrations are found near the ends of the overlap region [3]. Attempts have been made to reduce these concentrations by the introduction of a relatively compliant adhesive near the end region [4, 5]. Some of the recent research performed numerical analysis using finite element (FE) method on the single-lap aluminium bonded joints in the presence of a bi-adhesive bondline, and concluded that the presence of softer adhesive significantly reduces the stress concentration in the adhesive layer [6]. Significant performance enhancement of the 3D printed bondlayer tailored lap joints in terms of load carrying capacity and toughness as a result of single-step variation in modulus of the adhesive was reported in comparison to joints with homogenous adhesives [7]. Although analytical models for the stress-state prediction are developed for tubular bonded lap joints with homogeneous [8, 9] and functionally graded adhesives [10], numerical studies based on finite element (FE) analysis is generally adopted to study the behaviour of joints with bi-adhesive bondline [6, 11]. To the authors' best knowledge, there is no reported study for the evaluation of stresses in case of composite tubular bonded joints containing a bi-adhesive bondline. Das et al., [12-14] performed FE study on the tubular bonded joints comprising graphite epoxy FRP composite tubes in the presence of axial, pressure and torsional loading. The objective of this study is to extend this FE analysis, to study the behaviour of bi-adhesive bondline bonding composite FRP pipes under the action of axial, pressure and torsional loading.

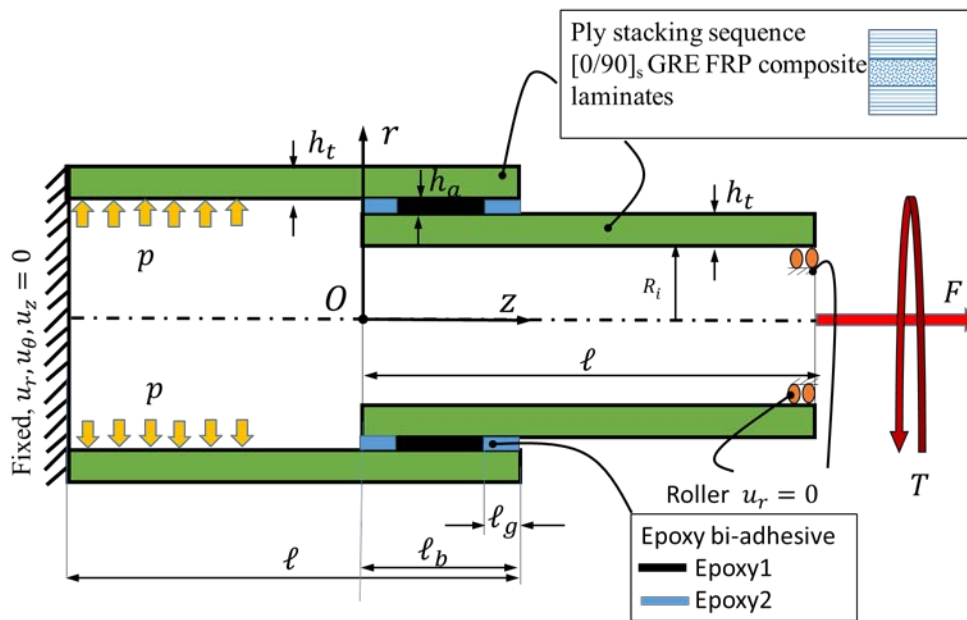


Figure 1: Schematic of the tubular bonded joint; longitudinal section of tubes bonded with bi-adhesive bondline subjected to axial load  $F$ , Torsion  $T$  and internal pressure  $p$ . Here  $l$ ,  $l_b$  represents the total length of the tube and the bonded overlap respectively while  $l_g$  represents the length of the compliant adhesive.

## 2. GEOMETRIC, MATERIAL AND BOUNDARY CONDITIONS

Tubular bonded joints comprising two GR/E  $[0/90]_s$  laminated FRP composite tubes is glued through a bi-adhesive bondline (see Table. 1 for properties). The inside radius of the inner tube ( $R_i = 18.9$  mm), thickness of both the tubes and the adhesive ( $h_t = 1$  mm,  $h_a = 0.15$  mm) and length of each adherend ( $l = 80$  mm) have been kept constant throughout the analyses. The geometric and material properties and

the loading conditions for the tubular adhesive bonded joints with homogeneous adhesive are taken from Das and Pradhan [13] and are shown in Fig. 1. The outer tube is fully restrained at tube overhang portion on the left-end while the inner tube is radially constraint at the right end. The axial and torsional loading is applied at the right end at the inner tube surface with the help of traction boundary conditions. An axial traction ( $\sigma_0$ ) of 10 MPa and a shear traction ( $\tau_s$ ) of 5 MPa is applied in case of axial and torsional loading on the inner tube overhang end. In case of pressure loading, an internal pressure ( $p$ ) of 1 MPa is applied at the inner surface of tubes (See Fig. 1).

Table 1: Material properties of the composite tubes and the Epoxy adhesives [14]

Joint materials	Constitutive behaviour	Young's modulus and Poisson's ratio
T 300/934 graphite/epoxy FRP tube	Orthotropic	$E_r = 4.8$ GPa, $E_\theta = 9.0$ GPa, $E_z = 127.5$ GPa $\nu_{zr} = \nu_{z\theta} = 0.28$ , $\nu_{\theta r} = 0.41$
Epoxy-1 stiff	Isotropic	$E = 2.8$ GPa, $\nu = 0.4$
Epoxy-2 compliant	Isotropic	$E = 1.0$ GPa, $\nu = 0.4$

### 3. FINITE ELEMENT (FE) MODELLING

3D FE models for composite tubular joints with the geometric and material properties discussed in the preceding section, was created in commercial code Abaqus version 6.14. A composite layup was created for the pipe section with the orthotropic properties given in Table. 1, and the stacking sequence of  $[0/90/0]_s$ . Plies are stacked radially where a ply with uni-directional fibres oriented in circumferential direction is considered as a zero degree ply while the ply oriented in axial direction is considered as a 90 degree ply. For simulating the bi-adhesive bondline, the adhesive was assigned with stiff epoxy-1 in the middle region and the compliant epoxy-2 in the end zones. The stiff epoxy-1 is used to simulate the homogenous adhesive for the baseline case.

Fig. 2a shows the full mesh in case of axial and pressure loading while a detailed view of the mesh near the overlap ends is seen in Fig. 2b. The 8-noded quadratic solid brick element with reduced integration (C3D8R) was used to model the adherends, consisting of three elements along the thickness which is equal to number of plies. Element size of 1 mm x 0.33 mm x 0.33 mm was used for the inner and outer tubes in the overhang region, away from the stress concentration zone. A stress concentration zone is found typically near the overlap ends of the joint in both the adherends and the adhesive. Element size in the mid overlap region was 0.33 mm x 0.33 mm x 0.33 mm while in the stress concentration zone it was refined to 0.1 mm x 0.33 mm x 0.33 mm [15]. A 8-noded linear solid element (C3D8R) was used for meshing the adhesive with four elements along the thickness ([12] suggested two elements along thickness). The adhesive was meshed with 0.33 mm x 0.33 mm x 0.33 mm sized elements and 0.1 mm x 0.33 mm x 0.33 mm in the mid-overlap region and the stress concentration zone respectively. A refined mesh was adopted in the overlap region to capture the stress gradients accurately. In case of axial and pressure loading, taking advantage of the symmetry, only a quarter cylinder of the tubes was modelled, with symmetry boundary conditions shown in Fig. 2c. The out-of-plane shear and radial stresses ( $\sigma_{rz}$ ,  $\sigma_{rr}$ ) are dominant in case of pure axial loading while additionally hoop stresses are dominant ( $\sigma_{\theta\theta}$ ) in case of pressure loading.

In case of torsional loading, full 3D model with complete tube geometry was modelled. A linear-static analysis was performed to evaluate the critical adhesive shear and radial stresses. In-plane shear stress component ( $\sigma_{r\theta}$ ) is dominant in case of torsional loading [12, 13]. It is important to note that the dominant stress components in each of the loading cases above is axisymmetric with respect to axis of the cylinder although material and loading conditions may not be axisymmetric.

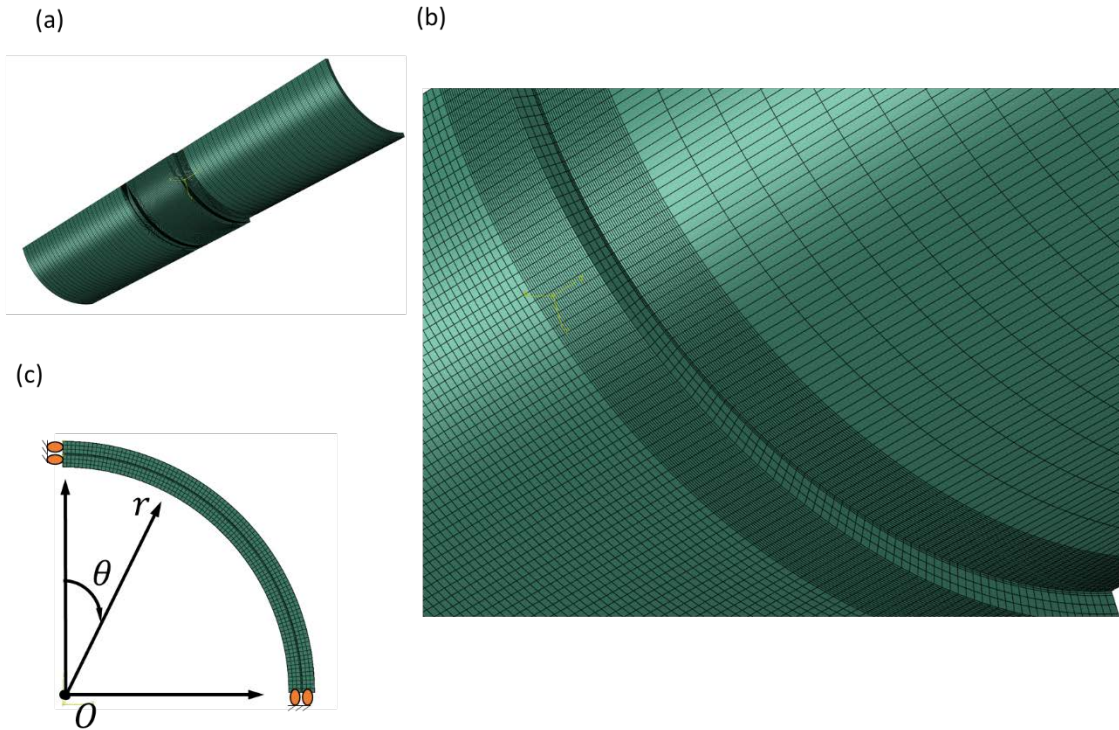


Figure 2: Finite element model for axial and pressure loading; (a). Full scale mesh (b). Details of the mesh near the overlap ends and (c) Cross-section of the mesh where symmetry conditions are applied. Note that the above model is only valid for axial and internal pressure loading. For torsional loading full scale 3D model without symmetry condition is created with a similar mesh.

#### 4. RESULTS AND DISCUSSIONS

Fig. 3 show the out-of-plane shear and radial stresses in the adhesive in case of pure axial loading of  $\sigma_a = 10$  MPa for the joints with homogeneous bondline with overlap length of  $l_b = 22$  mm. The shear and radial stress distribution obtained can be validated from the predictions of Das and Pradhan [12]. The obtained stress distributions are axisymmetric and hence plotted only along the axial direction. A region of zero shear stress in the bondline suffice the condition that the full shear transfer has occurred through the bondline. The shear stress distribution obtained in the Fig. 3a is devoid of any zero stress region along the bondline, indicating the absence of full load-transfer in shear. Hence we need to study the system at larger bondlength. Therefore, for the case for axial and pressure loading,  $l_b = 40$  mm was found to be appropriate for the complete shear transfer which can be confirmed from its shear stress distribution. Fig. 4 shows the shear and radial stress distributions along the mid-surface of the adhesive as a function of length of compliant region  $l_g$  in case of pure axial loading. The shear stress concentration reduces by about 35 % as the compliant region  $\frac{l_g}{l_b}$  increases upto 0.075 due to favourable redistribution of stresses owing to the presence of compliant adhesive as can be seen in Fig. 4a. Increasing the compliant region further the shear stress peaks increases, indicating that the optimal  $l_g$  should be chosen smaller for the parameters chosen here. Fig 4b shows that the radial stress peaks are reduced by about 45 % in presence of bi-adhesive bondlines as compared to the homogenous bondline and is same for a range of  $\frac{l_g}{l_b} = \{0.075, 0.125, 0.175\}$ .

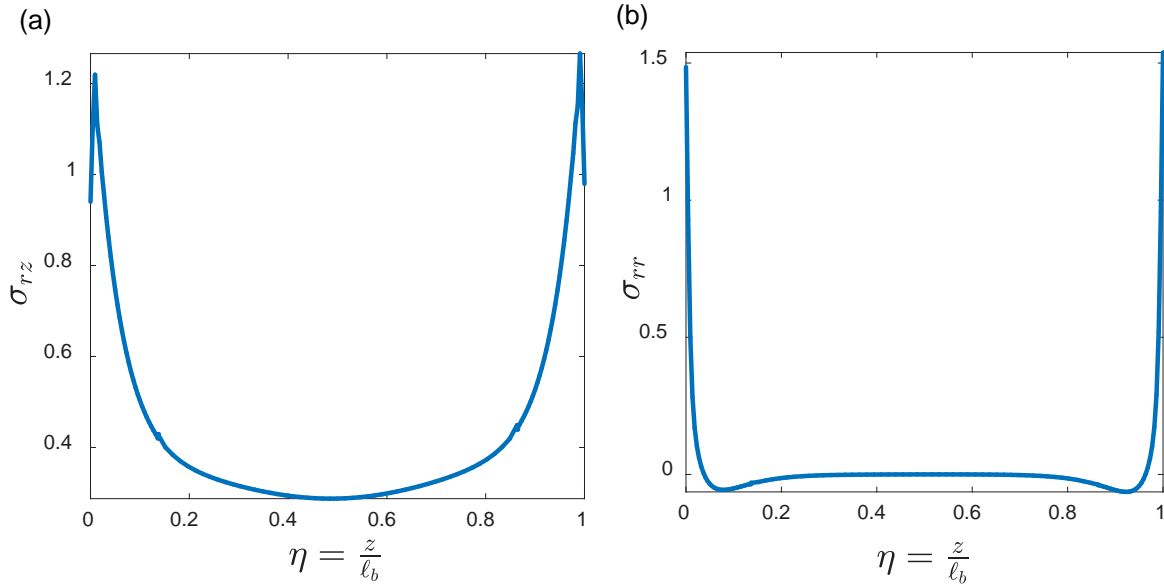


Figure 3: shear and radial stress distribution at the mid-surface of the tubular bonded joint for an overlap length of 22 mm and a homogenous adhesive. These predictions are in good agreement with [12].

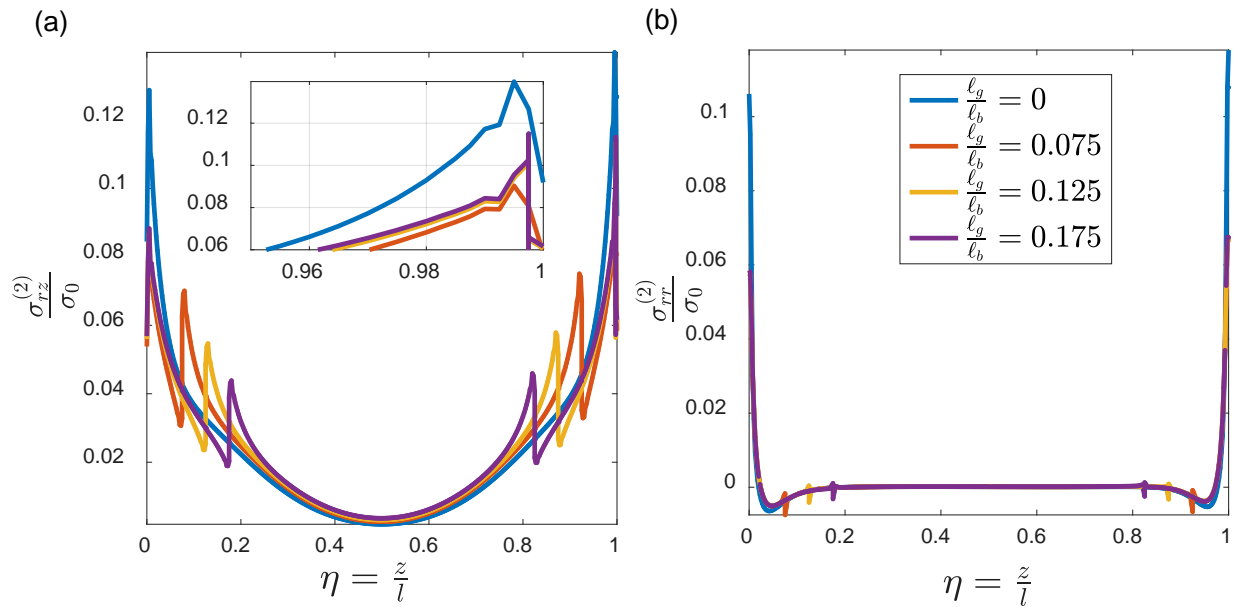


Figure 4: Shear and radial stress distribution at the mid-surface of the bi-adhesive as a function of length of compliant region  $\ell_g$  in case of pure axial loading with applied stress  $\sigma_0$ .

For the case of pure internal pressure loading, peak out-of-plane shear and peel stresses reduces by about 45 % and 40 % respectively in the presence of bi-adhesive bondline as can be seen in Fig. 5a and 5b. As an internal pressure is applied, the dominant effect of lateral deformation of the adherends inculcates additional stress concentration which can be easily relaxed by the use of bi-adhesive. From Fig. 5c, hoop stress concentration reduces by about 50 % due to the presence of bi-adhesive bondline. Shear, radial and hoop stress concentrations are almost constant for bi-adhesive containing softer adhesive of length  $\frac{\ell_g}{\ell_b} =$

{0.075, 0.125, 0.175}. Therefore, presence of bi-adhesive in case of internal pressure loading relaxes stress concentration peaks.

In case of pure torsional loading,  $\ell_b = 22$  mm was found to be enough for complete stress transfer. Since a full scale model was considered for the analysis, to optimize the computational model size, overlap length of  $\ell_b = 22$  mm was chosen with a bi-adhesive containing  $\ell_g = 3$  mm softer region. Normalized in-plane shear stress  $\tau_{r\theta}$  obtained in case of pure torsional loading is plotted in Fig. 6 for an overlap length of  $\ell_b = 22$  mm and compliant zone region  $\frac{\ell_g}{\ell_b} = 0.137$ . It can be clearly seen that the stress concentration peak is reduced by about 30 % in this case.

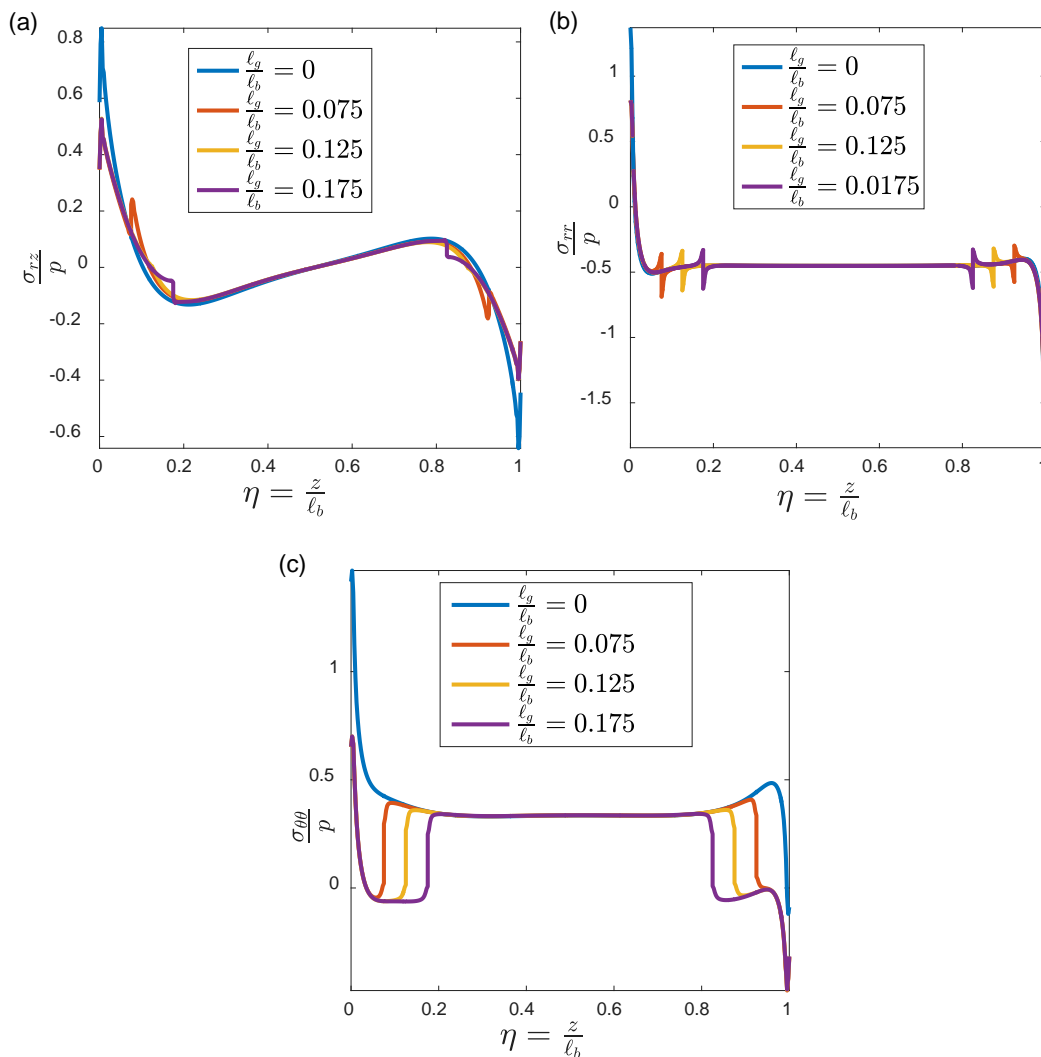


Figure 5: shear, radial and hoop stresses at the mid-surface of the bi-adhesive bondline as a function of length of compliant region  $\ell_g$  in case of pure internal pressure loading  $p$ .

## 5. CONCLUSION

A finite element analysis has been carried out for the composite tubular bonded joints considering ply stacking orientations using solid brick elements to model bonded composite tubes subjected to axial, pressure and torsional loading. The developed model is used to study the behaviour of composite bonded tubular lap joints containing two adhesives and found that the presence of compliant adhesive in all the loading case reduces the stress concentrations. In case of pure axial loading, peak shear and radial stresses reduce by 35% and 45% respectively in the presence of bi-adhesive bondline. For the case of pure internal pressure loading, peak shear, radial and hoop stresses reduce by 45%, 40% and 50% respectively in the presence of bi-adhesive bondline. In-plane shear stress concentration in case of pure torsional loading reduces by 30%.

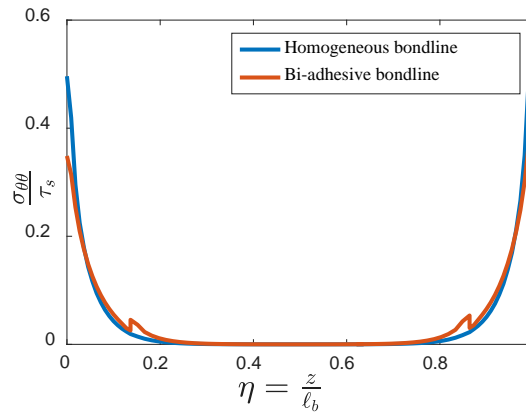


Figure 6: Normalized shear stress distribution for the case of torsional loading for a gradation length  $\frac{l_g}{l_b} = 0.137$  in case of pure torsion loading with applied shear torsion  $\tau_s$ .

## REFERENCES

- [1] A. Parashar and P. Mertiny, "Adhesively bonded composite tubular joints: review," *International Journal of Adhesion and Adhesives*, vol. 38, pp. 58-68, 2012.
- [2] S. J. Marshall, S. C. Bayne, R. Baier, A. P. Tomsia, and G. W. Marshall, "A review of adhesion science," *dental materials*, vol. 26, pp. e11-e16, 2010.
- [3] S. Kumar and M. Khan, "An elastic solution for adhesive stresses in multi-material cylindrical joints," *International Journal of Adhesion and Adhesives*, vol. 64, pp. 142-152, 2016.
- [4] L. F. da Silva and M. J. C. Lopes, "Joint strength optimization by the mixed-adhesive technique," *International Journal of Adhesion and Adhesives*, vol. 29, pp. 509-514, 2009.
- [5] S. Kumar and P. Pandey, "Behaviour of bi-adhesive joints," *Journal of Adhesion Science and Technology*, vol. 24, pp. 1251-1281, 2010.
- [6] I. Pires, L. Quintino, and R. Miranda, "Numerical simulation of mono-and bi-adhesive aluminium lap joints," *Journal of adhesion science and technology*, vol. 20, pp. 19-36, 2006.
- [7] S. Kumar, B. L. Wardle, and M. F. Arif, "Strength and Performance Enhancement of Bonded Joints by Spatial Tailoring of Adhesive Compliance via 3D Printing," *ACS Applied Materials & Interfaces*, 2016.
- [8] J. Lubkin and E. Reissner, *Stress distributions and design data for adhesive lap joints between circular tubes*: American Society of Mechanical Engineers, 1955.

- [9] L. Goglio and D. S. Paolino, "Adhesive stresses in axially-loaded tubular bonded joints—Part II: Development of an explicit closed-form solution for the Lubkin and Reissner model," *International Journal of Adhesion and Adhesives*, vol. 48, pp. 35-42, 2014.
- [10] S. Kumar, "Analysis of tubular adhesive joints with a functionally modulus graded bondline subjected to axial loads," *International Journal of Adhesion and Adhesives*, vol. 29, pp. 785-795, 2009.
- [11] H. Özer and Ö. Öz, "Three dimensional finite element analysis of bi-adhesively bonded double lap joint," *International Journal of Adhesion and Adhesives*, vol. 37, pp. 50-55, 2012.
- [12] R. Das and B. Pradhan, "Adhesion failure analyses of bonded tubular single lap joints in laminated fibre reinforced plastic composites," *International Journal of Adhesion and Adhesives*, vol. 30, pp. 425-438, 2010.
- [13] N. Baishya, R. R. Das, and S. Panigrahi, "Failure analysis of adhesively bonded tubular joints of laminated FRP composites subjected to combined internal pressure and torsional loading," *Journal of Adhesion Science and Technology*, pp. 1-25, 2017.
- [14] R. Das and B. Pradhan, "Finite element based design and adhesion failure analysis of bonded tubular socket joints made with laminated FRP composites," *Journal of Adhesion Science and Technology*, vol. 25, pp. 41-67, 2011.
- [15] P. Upadhyaya and S. Kumar, "Micromechanics of stress transfer through the interphase in fiber-reinforced composites," *Mechanics of Materials*, vol. 89, pp. 190-201, 2015.